Parameter Matching Using Adaptive Synchronization of Two Chua's Oscillators: MATLAB and SPICE Simulations

Valentin Siderskiy and Vikram Kapila

NYU Polytechnic School of Engineering, 6 MetroTech Center, Brooklyn, NY, USA
(E-mail: siderskiy@nyu.edu, vkapila@nyu.edu)

Abstract. In this paper, we use an adaptive synchronization technique for parameter matching with chaotic persistent excitation (PE). Two Chua's oscillators, identical in every parameter except for one, are set up in a master/slave configuration where the slave's mismatched parameter is adaptable. Using a Lyapunov function and incorporating the presence of PE, an adaptive control law is given to ensure exact parameter matching. A high-fidelity SPICE simulation model is given that incorporates commercially-provided macro models of the integrated circuits used and obviates the need for any user-defined functions. A voltage controlled inductor-gyrator is used as a tunable parameter made up of current feedback op amps (CFOAs). The performance of the adaptive controller is compared over a wide range of parameter values by using MATLAB simulations. SPICE and MATLAB simulations are run with realistic component tolerances to mimic a physical experiment.

Keywords: Chua's oscillator, adaptive synchronization, parameter matching, inductor-gyrator, CFOA, chaotic simulation, SPICE, MATLAB, TINA-TI.

1 Introduction

Chua's circuit has been extensively used to study various topics relating to chaos theory, including synchronization of coupled chaotic systems [13]. When two chaotic systems are not identical, synchronization becomes less trivial and various adaptive schemes are considered. For example, adaptive synchronization of Chua's oscillator has been considered with adaptive observer design [5], parameter identification [19], and adaptive backstepping [6]. Many of the prior works are theoretical in nature, difficult to realize experimentally, and may not yield exact parameter matching [3]. To render adaptive synchronization of chaotic circuits closer to physical realization, Ref. [18] has provided SPICE simulations with ideal user defined functions for the adaptive controller. Ref. [8] has suggested circuit schematics to realize an adaptive controller for synchronization of uncertain and delayed chaotic systems, but it does not account for the non-ideal characteristics of integrated circuits such as the AD633.

7th CHAOS Conference Proceedings, 7-10 June 2014, Lisbon Portugal
C. H. Skiadas (Ed)

Adaptive synchronization of Chua's oscillators can be categorized in two parts: adapting the control coupling between the two circuits or adapting one or more parameters of the Chua's oscillators [4]. Both adaptive synchronization approaches have been digitally implemented for secure communication applications. The first approach is used to account for changes in signal strength [20], while the second approach introduces deliberate changes in the parameters as a way to send binary messages as a 'key' [4].

In this paper, we use an adaptive synchronization technique for parameter matching with chaotic PE. Two Chua's oscillators, identical in every parameter except for one, are set up in a master/slave configuration where the slave's mismatched parameter is adaptable. Using a Lyapunov function and incorporating the presence of PE, an adaptive control law is given to ensure exact parameter matching. Following Ref. [15], this paper uses analog circuit schematics, which exploit CFOAs, to implement the derived adaptive controller. Moreover, a high-fidelity SPICE simulation model is provided that incorporates commercially available macro models of various integrated circuits used and obviates the need for any user-defined functions. The performance of the adaptive controller is compared over a wide range of parameter values by using MATLAB simulations. SPICE and MATLAB simulations are run with realistic component tolerances to mimic a physical experiment. For experimental results that parallel the simulation studies of this paper, see Ref. [15].

2 System Model

2.1 Chua's Oscillator

In this paper, an adaptive controller is designed to tune a parameter of the Chua's oscillator shown in Figure 1. Various parameters of a Chua's oscillator include L as a linear inductor, R and R_0 as linear resistors, C_1 and C_2 as linear capacitors, and others that correspond to the Chua's diode. The state equations of the Chua's oscillator are given by

$$\begin{aligned} \frac{\mathrm{d}v_1}{\mathrm{d}t} &= \frac{1}{C_1}\Big(G\,(v_2 - v_1) - g\,(v_1)\Big), \\ \frac{\mathrm{d}v_2}{\mathrm{d}t} &= \frac{1}{C_2}\Big(G\,(v_1 - v_2) + i_L\Big), \qquad \frac{\mathrm{d}i_L}{\mathrm{d}t} = \frac{1}{L}\,(-v_2 - R_0 i_L)\,, \end{aligned} \tag{1}$$

where v_1, v_2, and i_L are voltage across C_1, voltage across C_2, and current through L, respectively, and G is the conductance of the resistor R ($G \triangleq \frac{1}{R}$). Furthermore $g(\cdot)$ is the nonlinear voltage-current (v–i) characteristic of the Chua's diode described by

$$g(v_R) = \begin{cases} G_b v_R + (G_b - G_a)E_1, & \text{if } \ v_R \ \leq -E_1, \\ G_a v_R, & \text{if } |v_R| < E_1, \\ G_b v_R + (G_a - G_b)E_1, & \text{if } \ v_R \ \geq E_1, \end{cases} \tag{2}$$

where G_a, G_b, and E_1 are known real constants that satisfy $G_b < G_a < 0$ and $E_1 > 0$.

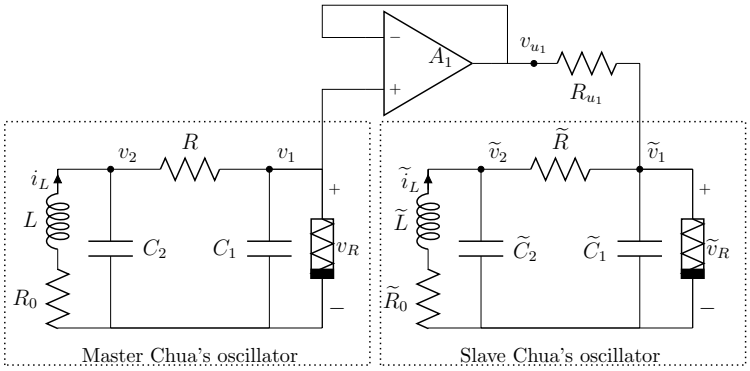

Fig. 1. Master/slave Chua's oscillator coupling.

2.2 Master/slave System

The adaptive control framework of this paper considers a unidirectional coupling from a master Chua's oscillator to a slave Chua's oscillator such that the slave Chua's oscillator synchronizes its states to the states of the master oscillator which operates autonomously. This configuration is shown in Figure 1 where it is assumed that the following parameters of the master and slave Chua's oscillators are matched, $\widetilde{R} = R$, $\widetilde{R}_0 = R_0$, $\widetilde{C}_1 = C_1$, and $\widetilde{C}_2 = C_2$. The state equations of the master Chua's oscillator are equivalent to (1) while the state equations of the slave Chua's oscillator are given by

$$\begin{aligned} \frac{\mathrm{d}\widetilde{v}_1}{\mathrm{d}t} &= \frac{1}{C_1}\Big(G(\widetilde{v}_2 - \widetilde{v}_1) - g(\widetilde{v}_1) + G_{u_1}(v_{u_1} - \widetilde{v}_1)\Big), \\ \frac{\mathrm{d}\widetilde{v}_2}{\mathrm{d}t} &= \frac{1}{C_2}\left(G\left(\widetilde{v}_1 - \widetilde{v}_2\right) + \widetilde{i}_L\right), \qquad \frac{\mathrm{d}\widetilde{i}_L}{\mathrm{d}t} = \frac{1}{\widetilde{L}}(-\widetilde{v}_2 - R_0\widetilde{i}_L), \end{aligned} \tag{3}$$

where $v_{u_1} = v_1$ since it is the output of a voltage follower op-amp and G_{u_1} is the conductance of the coupling resistor R_{u_1} in Figure 1 ($G_{u_1} \triangleq \frac{1}{R_{u_1}}$). Note that $\widetilde{L}$ is a tunable parameter for which we give an adaptive parameter update law in Section 3.

3 Adaptive Synchronization: Tuning $\widetilde{L}$

In a master/slave configuration, the master Chua's oscillator is described by (1). For the slave Chua's oscillator, inductance $\widetilde{L}$ is the tunable mismatched parameter for the slave Chua's oscillator (3). Subtracting (1) from (3) produces the error dynamics

$$\begin{aligned} \dot{e}_{v_1} &= \frac{1}{C_1}\Big(G\left(e_{v_2} - e_{v_1}\right) - c\left(\widetilde{v}_1, v_1\right)e_{v_1} + u_1\Big), \\ \dot{e}_{v_2} &= \frac{1}{C_2}\Big(G\left(e_{v_1} - e_{v_2}\right) + e_{i_L}\Big), \quad \dot{e}_{i_L} = \frac{1}{\widetilde{L}}(-\widetilde{v}_2 - R_0\widetilde{i}_L) + \frac{1}{L}\left(v_2 + R_0 i_L\right), \end{aligned} \tag{4}$$

where $e_{v_1} \triangleq \widetilde{v}_1 - v_1$, $e_{v_2} \triangleq \widetilde{v}_2 - v_2$, and $e_{i_L} \triangleq \widetilde{i}_L - i_L$ are the error states and $u_1 \triangleq G_{u_1}(v_1 - \widetilde{v}_1)$. Moreover, it is easy to show that $g(\widetilde{v}_1) - g(v_1) = c(\widetilde{v}_1, v_1)e_{v_1}$ where $c(\widetilde{v}_1, v_1)$ is bounded by the constraints $G_a \leq c(\widetilde{v}_1, v_1) \leq G_b < 0$ [7].

Next, let the control law and parameter update law, respectively, be given by

$$u_1 = -G_{u_1} e_{v_1} \qquad \text{and} \qquad \frac{\mathrm{d}}{\mathrm{d}t}\left(\frac{1}{\widetilde{L}}\right) = \gamma e_{i_L}\left(\widetilde{v}_2 + R_0 \widetilde{i}_L\right), \tag{5}$$

where γ is a positive constant.

Theorem 1. **[15]** *The two Chua's oscillators (1) and (3) will synchronize and the parameter $\widetilde{L}$ will converge to some constant under (5) if the master system (1) remains on the trajectory of its chaotic attractor and G_{u_1} is chosen to satisfy the following inequality*

$$G_{u_1} > \frac{1}{2}G - G_a. \tag{6}$$

Remark 1. Note that the results of Theorem 1 are also applicable if the Chua's oscillator is on a periodic trajectory. As long as the attractor of the Chua's oscillator is bounded, the results of Theorem 1 hold.

Remark 2. When the trajectories of (1) are driven on a chaotic attractor, its states will satisfy the qualities of PE as discussed in [10,11,14] and $\widetilde{L}(t) \to L(t)$ as $t \to \infty$. Further evidence of $\widetilde{L}(t) \to L(t)$ as $t \to \infty$ is provided via simulation results in the sequel.

4 Tuning $\widetilde{L}$ Implementation

Over the years, several variations of the Chua's oscillators have been developed [9]. Similarly, master/slave coupling between two Chua's oscillators for state v_1 (and v_2) is easily achievable with just one resistor and one op-amp (Figure 1). However, measuring and controlling the state i_L is not as trivial. Therefore variations of inductorless implementations of Chua's oscillators have been developed [9]. This paper implements the adaptive controller (5) which tunes the parameter $\widetilde{L}$ to L. The measurement of i_L and $\widetilde{i}_L$ along with the ability to tune $\widetilde{L}$ is possible by using inductor-gyrators made up of CFOAs. Refer to our parallel experimental work [15] for detailed explanation of the circuitry required for this task.

5 SPICE and MATLAB Simulation Results

5.1 SPICE Simulation Results

SPICE simulations are done to mimic an experimental scenario to examine the influence of unmodeled parasitic effects on the physical system that are not amenable to examination using the ideal circuit equations such as (1),

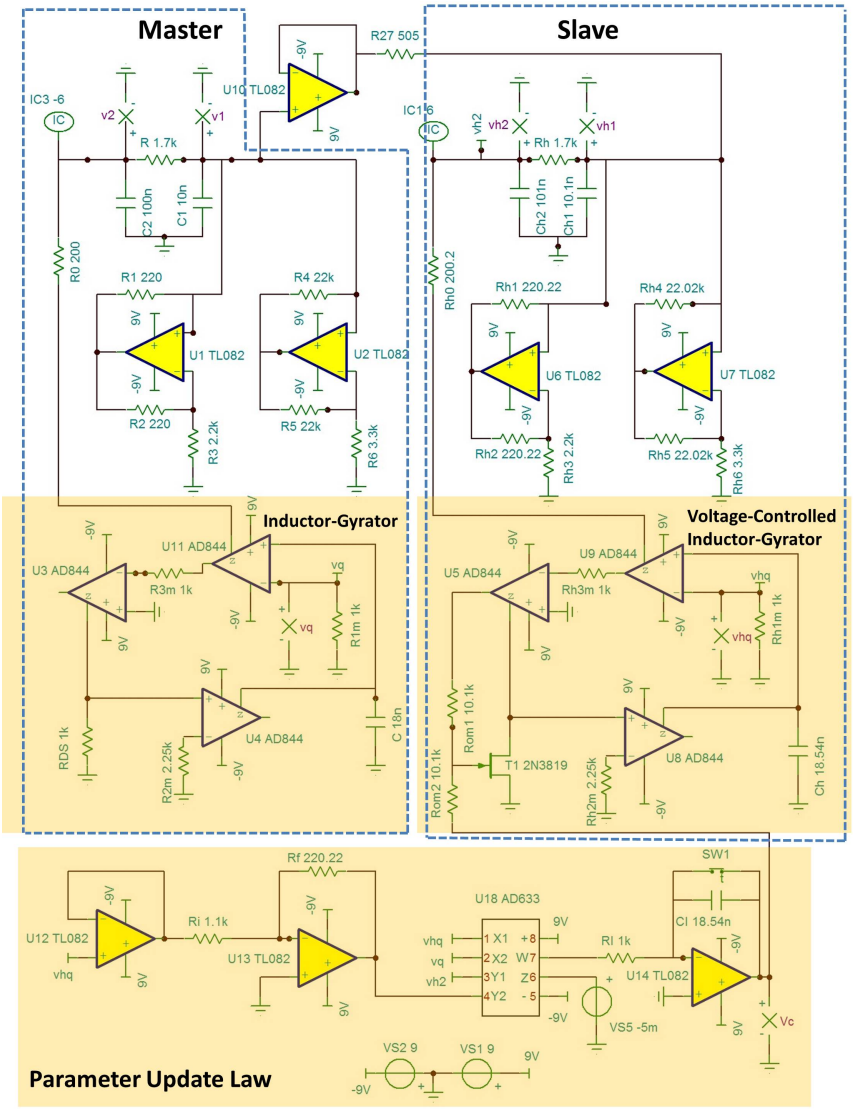

Fig. 2. Schematic of master/slave Chua's oscillator as constructed in the TINA-TI SPICE simulation software.

(3), and (5). This simulation strategy can be an integral step in designing complex chaotic experiments. Hence, we develop a SPICE simulation model (see Figure 2) containing the various non-ideal behaviors of components such that the simulation model can closely represent a plausible experiment. This includes extracting the signals i_L and $\widetilde{i}_L$ by measuring the voltages at nodes vq and vhq in the SPICE simulation (see Figure 2) as opposed to directly extracting i_L ($vq = i_L R_{1m}$) and $\widetilde{i}_L$ ($vhq = \widetilde{i}_L \widetilde{R}_{1m}$). The SPICE simulator TINA-TI V9 [16] is chosen because of the capability of its numerical solver

to optimize its tolerance parameters for convergence. As shown in Figure 2, we used three distinct integrated circuits (ICs), the AD633, the AD844, and the TL082. High fidelity SPICE Macro-Models [1, 2, 17] of each IC are used in the SPICE simulation. Similarly, the JFET used, the 2N3819, is modeled in TINA-TI V9 using the Sckickman-Hodges model with specific parameters for the 2N3819 already embedded in the software. Simulation is run using the order 2 trapezoidal integration method. Two initial conditions are set to -6V and 6V at nodes v_2 and $\widetilde{v}_2$, respectively. The AD633 input terminal Z has a direct -5 mV source connected to it for the purpose of compensating for the internal DC offset of the AD633.

The simulation uses the ideal values of the passive components for the master Chua's oscillator as shown in Table 1. In addition, values of passive components in the slave Chua's oscillator and adaptive controller are increased by their respective tolerances as indicated in Table 1. These tolerances are selected based on commercially available components.

Table 1. Simulation component values.

Master Chua's Oscillator	Adaptive Controller	Slave Chua's Oscillator
$R_1 = 22$ kΩ	$R_{u_1} = 500\ \Omega$ 1%	$\widetilde{R}_1 = 22$ kΩ 0.1%
$R_2 = 22$ kΩ	$R_I = 1$ kΩ 0.1%	$\widetilde{R}_2 = 22$ kΩ 0.1%
$R_3 = 3.3$ kΩ	$C_I = 18$ nF 3%	$\widetilde{R}_3 = 3.3$ kΩ 0.1%
$R_4 = 220\ \Omega$	$R_i = 1.1$ kΩ 0.1 %	$\widetilde{R}4 = 220\ \Omega$ 0.1%
$R_5 = 220\ \Omega$	$R_f = 220\ \Omega$ 0.1 %	$\widetilde{R}_5 = 220\ \Omega$ 0.1%
$R_6 = 2.2$ kΩ		$\widetilde{R}_6 = 2.2$ kΩ 0.1%
$R = 1.7$ kΩ		$\widetilde{R} = 1.7$ kΩ 0.1%
$C_1 = 10$ nF		$\widetilde{C}_1 = 10$ nF 1%
$C_2 = 100$ nF		$\widetilde{C}_2 = 100$ nF 1%
$C = 18$ nF		$\widetilde{C} = 18$ nF 3%
$R_0 = 200\ \Omega$		$\widetilde{R}_0 = 200\ \Omega$ 0.1 %
$R_{1m} = 1$ kΩ		$\widetilde{R}_{1m} = 1$ kΩ 0.1%
$R_{2m} = 2.25$ kΩ		$\widetilde{R}_{2m} = 2.25$ kΩ 0.1 %
$R_{3m} = 1$ kΩ		$\widetilde{R}_{3m} = 1$ kΩ 0.1%
$R_{DS} = 1$ kΩ		TR = 2N3819
		$\widetilde{r}_{om1} = 10$ kΩ 1%
		$\widetilde{r}_{om2} = 10$ kΩ 1%

To quantify how well the master/slave system synchronizes, we use the 2-norm of $[e_{v_1}, e_{v_2}, e_{i_L}]^{\mathrm{T}}$ as our measure, ($e_{\mathrm{norm}} \triangleq ||[e_{v_1}, e_{v_2}, e_{i_L}]^{\mathrm{T}}||$), and observe its evolution over time. Using the signals $\widetilde{i}_L$ and $\widetilde{v}_2$ we estimate $\widetilde{L}$ and $\widetilde{R}_0$ ($\widetilde{L}_{\mathrm{est}}$, $\widetilde{R}_{0\mathrm{est}}$) with a sliding window least square algorithm. Similarly, using signals i_L and v_2 we estimate L and R_0 (L_{est}, $R_{0\mathrm{est}}$). Comparing these estimates allows us to examine how well $\widetilde{L}$ converges to L. The transient experimental data is displayed in Figure 3, divided into parts (a)–(e). Switch SW1 is opened at $t = 0.025s$ which initiates adaptation. Each point on Figure 3(c) represents a least square estimate of a window of 50 samples and the x-axis indicates the time when the leading sample is taken. Figure 3(d) and Figure 3(e) re-plot the last 10 ms of Figure 3(b) and Figure 3(c), respectively, to better visualize the

steady-state results. The average of each signal (except V_c) in sections (d) and (e) is listed in Table 2.

Table 2. SPICE simulation: Adapting for $\widetilde{L}$ with tolerances.

$R_0 = 200\ \Omega$	$R_{0\text{est}} = 202.89\ \Omega$ (average)
$\widetilde{R}_0 = 200.2\ \Omega$	$\widetilde{R}_{0\text{est}} = 202.84\ \Omega$ (average)
$L = 40.5$ mH (see (21) [15])	$L_{\text{est}} = 45.4$ mH (average)
$e_{\text{norm}} = 1.8 \times 10^{-3}$ (average)	$\widetilde{L}_{\text{est}} = 45.3$ mH (average)

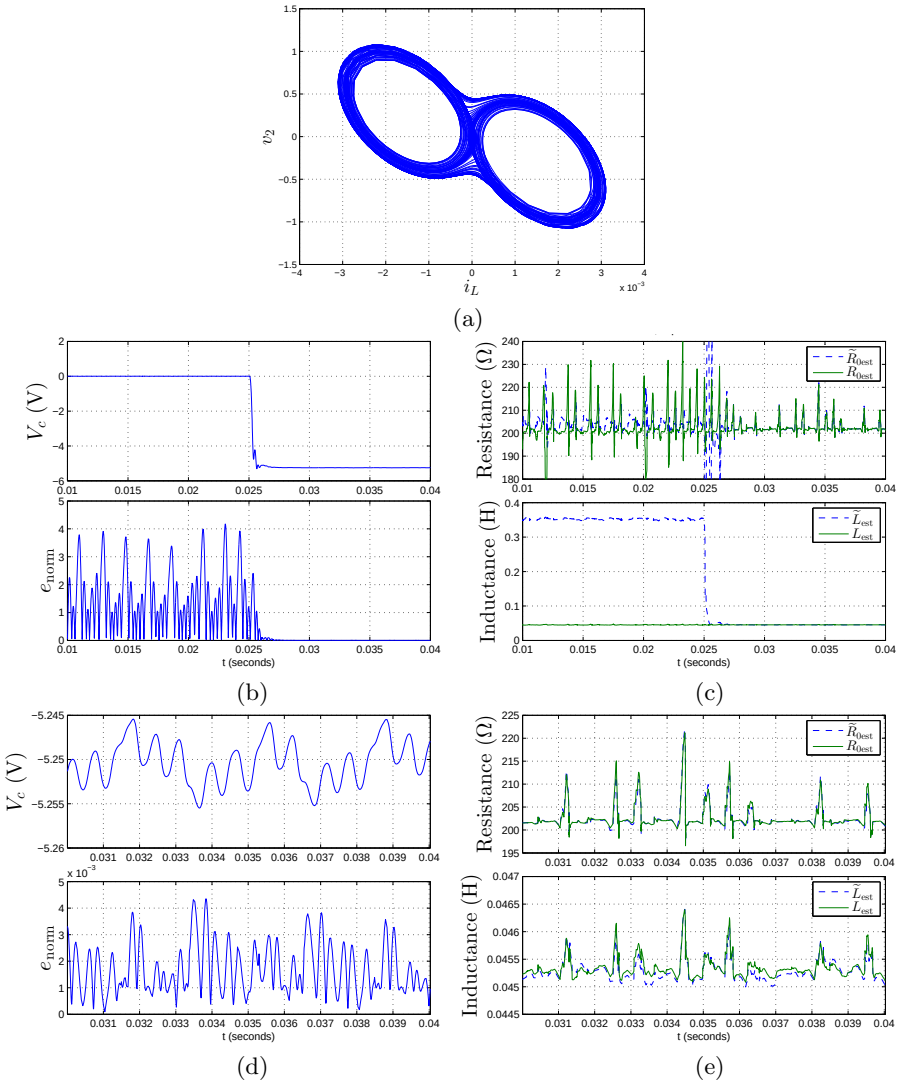

Fig. 3. SPICE simulation: Adapting for $\widetilde{L}$ with tolerances.

5.2 MATLAB Simulation Results

MATLAB-Simulink simulations are run to examine the performance of the adaptive control laws derived in Section 3 as a function of the behavior of the master Chua's oscillator which changes from chaotic to equilibrium behavior. Simulations are run 1,000 times for 1,000 different values of C_1 ranging from 10 nF to 13 nF. With each change in the C_1 value, the simulation result for the master Chua's attractor also changes. To illustrate the change in the master Chua's attractor with the change in the value of C_1, Figure 4 provides the bifurcation diagram for the master Chua's oscillator for the 1,000 values of C_1. To capture the impact of component tolerances the slave Chua's oscillator parameters are increased by 0.1% (not including $\widetilde{C}_1$, which is set to C_1).

All simulations are set up as follows: simulations are run by using the Runge-Kutta 4th order numerical solver with a fixed step-size of 10 microseconds for a simulation time of two seconds. The initial conditions are selected to be $v_1(0) = 1$, $v_2(0) = 0$, $i_L(0) = 0$, $\widetilde{v}_1(0) = 2$, $\widetilde{v}_2(0) = 0$, and $\widetilde{i}_L(0) = 0$. Since it takes time for the master Chua's oscillator to evolve from the initial condition to reach the attractor corresponding to the chosen C_1 value, the parameter update law is activated only after 0.5 seconds into the simulation. The parameters used in simulations are listed in Table 3. Figure 4 shows the results for the MATLAB simulation. Figure 4 uses three measures to examine the performance of the adaptive controller. The first performance measure is the error $e_\rho(t = 2)$, that is the parameter error after two seconds of simulation time averaged over the last 10 ms of simulation. The second performance measure is $e_{\text{norm}}(t = 2)$, that is the norm of the error state vector after two seconds of simulation time averaged over the last 10 ms of simulation. Finally, the third performance measure is the settling time (t_{st}), that is the time it takes the slave oscillator's adaptive parameter to reach within 10% of the master's corresponding fixed parameter.

Table 3. MATLAB simulation parameters.

G =1/1700 S	$\widetilde{G}$ =1/1700 + 1/1700000 S	$\gamma = 5 \times 10^7$
R_0 =13 Ω	$\widetilde{R}_0 = 13.013\ \Omega$	$L = 18$ mH
$G_a = -0.40909$ mS	$\widetilde{G}_a = -0.40949909$ mS	$\widetilde{L}(0) = 10$ mH
$G_b = -0.75758$ mS	$\widetilde{G}_b = -0.75833758$ mS	
E_1 =1.1739 V	$\widetilde{E}_1$ =1.1750739 V	
$G_{u_1} = 1/500$ S	G_{u_1} =1/500 + 1/500000 S	
$C_2 = 100$ nF	$\widetilde{C}_2 = 100.1$ nF	

5.3 Discussion

We first comment on the overall performance of the SPICE simulation performed in Section 5.1 by observing Figures 3(b) and 3(c). In the macro scale plot, once the adaptive controller is activated at $t = 0.025s$, the measure e_{norm} approaches zero and the estimates of the slave oscillator parameters ($\widetilde{R}_{\text{est}}$ and $\widetilde{L}_{\text{est}}$) approach the corresponding parameter values of the master oscillator. However, in Figure 3(c), estimated values of R_0 and $\widetilde{R}_0$ undergo change despite the fact that R_0 is a fixed parameter and the parameter update law is only

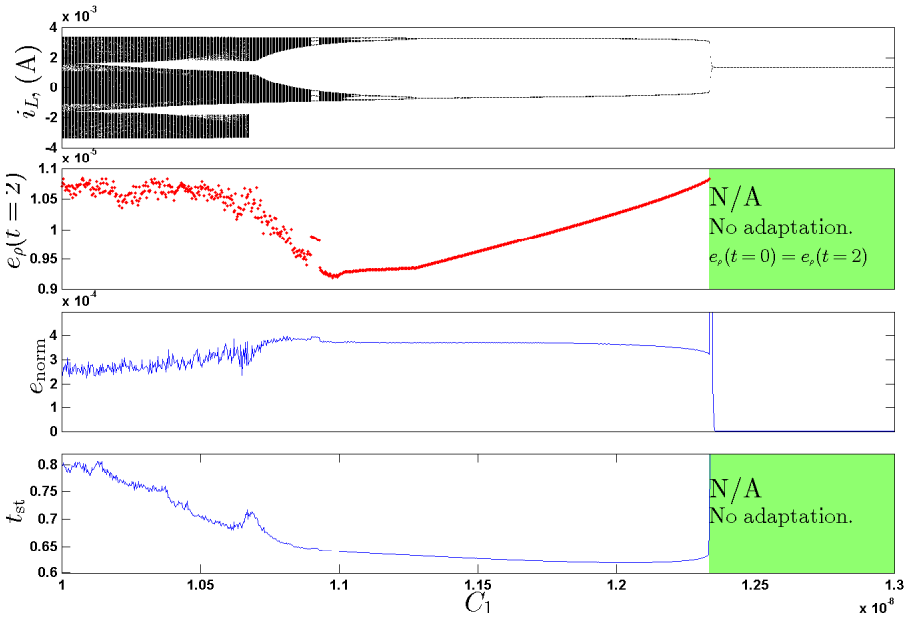

Fig. 4. MATLAB Simulation: Adapting for $\widetilde{L}$ with tolerances.

supposed to change the parameter value $\widetilde{L}$. This indicates that the inductor-gyrator is not a pure inductor but only a good-enough model for this system to operate within certain tolerances. Next, we examine Figures 3(d) and 3(e) which show the last 10ms of Figures 3(b) and 3(c), respectively. The state errors between the master and slave Chua's oscillator still exist and the parameters L and $\widetilde{L}$ do not perfectly match, with a 0.1mH difference on average (Table 2). This mismatch is attributed to component tolerances. In a simulation study of adaptive synchronization of Chua's oscillators with a mismatched parameter, [12] similarly observed that the adaptive parameter does not converge to the desired value. Repeating the SPICE simulation without including competent tolerances (see Table 4 and Figure 5), it is seen by averaging the last 10 ms of the 40 ms simulation that there is no difference between L_{est} and $\widetilde{L}_{est}$.

Next, we comment on our MATLAB simulation results (Figure 4) that illustrate how the adaptive controller performs depending on the behavior of the master Chua's oscillator. Note that adaptation of parameter $\widetilde{L}$ occurs regardless of the system being chaotic or a simple oscillator. The adaptive controller stops working only when the master Chua's oscillator is in steady state. A close examination of Figure 4 reveals a large spike in e_{norm} at around $C_1 = 12.32$ nF. This spike is due to the fact that in this small range of C_1 the Chua's oscillator is approaching equilibrium very slowly in which the 2 second simulation time is not enough for the master Chua's oscillator to reach its steady state behavior. The only time e_{norm} reaches close to zero is when the Chua's attractor is in equilibrium, which is when C_1 goes above 12.33 nF. At equilibrium, the energy storing components no longer have a long term effect on the system and the

inductor functionally behaves as a short and the capacitors behave as open. In this mode, the adaptive parameters do not converge to any particular value but stay the same. Additional MATLAB simulations conducted with ideal parameter values show that the errors decrease by several orders of magnitude (see Figure 6).

Table 4. SPICE simulation: Adapting for $\widetilde{L}$ without tolerances.

$R_0 = 200\ \Omega$	$R_{0\text{est}} = 202.42\ \Omega$ (average)
$\widetilde{R}_0 = 200\ \Omega$	$\widetilde{R}_{0\text{est}} = 202.46\ \Omega$ (average)
$L = 40.5$ mH (see (21) [15])	$L_{\text{est}} = 45.4$ mH (average)
$e_{\text{norm}} = 1.6 \times 10^{-3}$ (average)	$\widetilde{L}_{\text{est}} = 45.4$ mH (average)

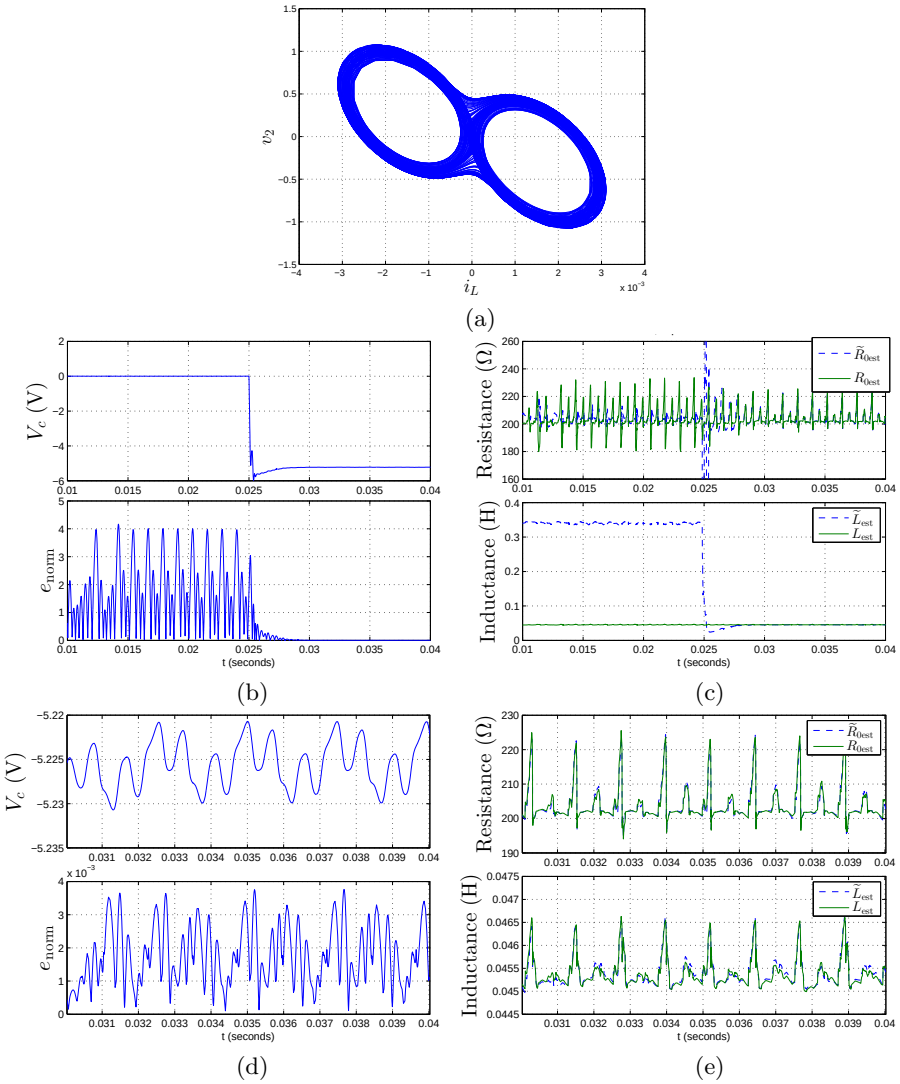

Fig. 5. SPICE simulation: Adapting for $\widetilde{L}$ without tolerances.

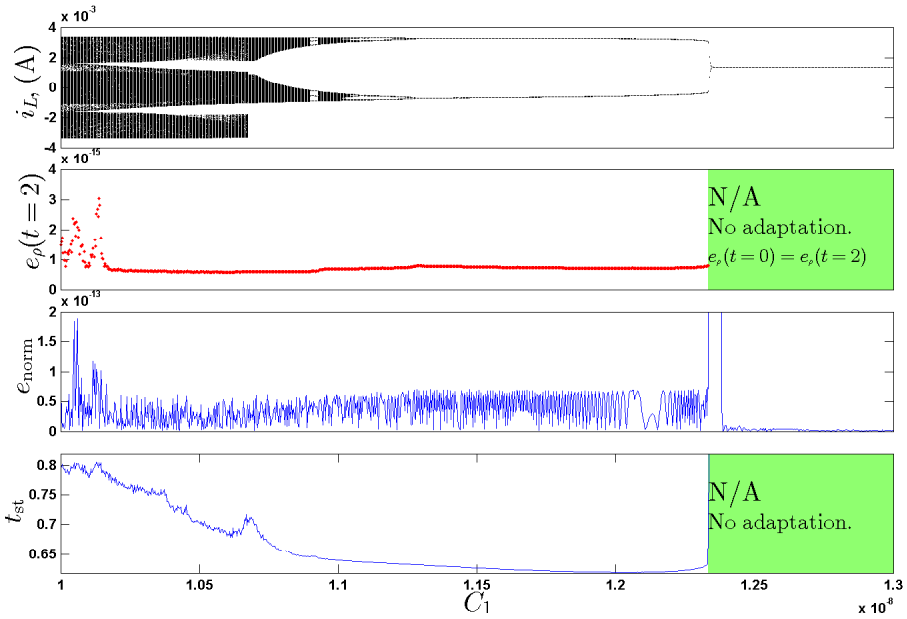

Fig. 6. MATLAB simulation: Adapting for $\widetilde{L}$ without tolerances.

6 Conclusion

In this paper we presented an adaptive controller that is designed to match a parameter (L) in two Chua's oscillators with the presence of PE. We implemented the adaptive controller using analog circuitry in a high-fidelity SPICE simulation while incorporating reasonable electrical component tolerances. Furthermore, we tested our adaptive controllers over many conditions of the Chua's oscillator using MATLAB simulations. Our results show that the adaptive controller achieves parameter matching with a certain degree of error due to tolerance mismatch of the master and slave Chua's oscillator. In addition, the adaptive controller performs not only when the master Chua's oscillator is in the chaotic mode but also when the system is a simple oscillator (and does not fulfill the qualities of PE).

Acknowledgements

This paper is supported in part by the following grants: NSF-EEC-1132482, NSF-DGE: 0741714, and NY Space Grant: 48240-7887.

References

1. Analog Devices, "AD633 analog multiplier macro model," www.analog.com/Analog_Root/static/techSupport/designTools/spiceModels/license/spice_general.html?cir=ad633.cir, 2012, accessed: 2014-3-25.

2. Analog Devices, "AD844 monolithic op amp," http://www.analog.com/Analog_Root/static/techSupport/designTools/spiceModels/license/spice_general.html?cir=ad844.cir, 2012, accessed: 2014-3-25.
3. S. Bowong, M. Kakmeni, and R. Koina, "Chaos synchronization and duration time of a class of uncertain chaotic systems," *Math. Comput. Simul*, vol. 71, no. 3, pp. 212–228, 2006.
4. L. O. Chua, *et al.*, "Adaptive synchronization of Chua's oscillators," *Int. J. Bifurcat. Chaos*, vol. 6, no. 1, pp. 189–201, 1996.
5. A. Fradkov and A. Markov, "Adaptive synchronization of chaotic systems based on speed gradient method and passification," *IEEE Trans. Circuits Syst. I, Fundam. Theory Appl*, vol. 44, no. 10, pp. 905–912, 1997.
6. S. Ge and C. Wang, "Adaptive control of uncertain Chua's circuits," *IEEE Trans. Circuits Syst. I, Fundam. Theory Appl*, vol. 47, no. 9, pp. 1397–1402, 2000.
7. A. Hegazi, H. Agiza, and M. El-Dessoky, "Adaptive synchronization for Rössler and Chua's circuit systems," *Int. J. Bifurcat. Chaos*, vol. 12, no. 7, pp. 1579–1597, 2002.
8. X.-Z. Jin, W. W. Che, and D. Wang, "Adaptive synchronization of uncertain and delayed chaotic systems with its circuit realization," in *Proc. of World Cong. Intelligent Control and Automation*, 2012, pp. 3465–3470.
9. R. Kilic, *A practical guide for studying Chua's circuits.* In World Scientific Series on Nonlinear Science, World Scientific, 2010, vol. 71.
10. K.-Y. Lian, *et al.*, "Adaptive synchronization design for chaotic systems via a scalar driving signal," *IEEE Trans. Circuits Syst. I, Fundam. Theory Appl*, vol. 49, no. 1, pp. 17–27, 2002.
11. K. Narendra and A. Annaswamy, *Stable adaptive systems.* Dover Publications, 2005.
12. U. Parlitz and L. Kocarev, "Multichannel communication using autosynchronization," *Int. J. Bifurcat. Chaos*, vol. 6, no. 3, pp. 581–588, 1996.
13. L. M. Pecora and T. L. Carroll, "Synchronization in chaotic systems," *Phys. Rev. Lett.*, vol. 64, pp. 821–824, 1990.
14. S. Sastry and M. Bodson, *Adaptive control: stability, convergence and robustness.* Dover Publications, 2011.
15. V. Siderskiy and V. Kapila, "Parameter matching using adaptive synchronization of two Chua's oscillators," in *Proc. of the 2014 American Control Conf., 2014.*
16. Texas Instruments. "Getting started with TINA-TI," http://www.ti.com, 2008, accessed: 2014-3-25.
17. Texas Instruments, "TL082 SPICE macro-model," http://www.ti.com/product/tl082, 2013, accessed: 2014-3-25.
18. M. Xiao and J. Cao, "Synchronization of a chaotic electronic circuit system with cubic term via adaptive feedback control," *Commun. Nonlinear Sci. Numer. Simul.*, vol. 14, no. 8, pp. 3379 – 3388, 2009.
19. J. Zhou, T. Chen, and L. Xiang, "Adaptive synchronization of coupled chaotic delayed systems based on parameter identification and its applications," *Int. J. Bifurcat. Chaos*, vol. 16, no. 10, pp. 2923–2933, 2006.
20. H. Zhu and B. Cui, "A new adaptive synchronization scheme of delayed chaotic system for secure communication with channel noises," in *Proc. of Int. Conf. Computer Design and Applications*, vol. 4, 2010, pp. V4–433–437.